Research Square

Preprints are preliminary reports that have not undergone peer review.
They should not be considered conclusive, used to inform clinical practice,
or referenced by the media as validated information.

AI-Based Inline PCB Defect Detection and Robotic Sorting Using Smart Vision, PLC Logic, Fanuc Vision and SCADA Integration

Mizengo Abel Kabwe
Michigan Technological University College of Computing
Jacob Fata
Michigan Technological University College of Computing
Ikerbold Nyasha Muzanenhamo
Michigan Technological University College of Computing
Cecil Takunda Mhike
Michigan Technological University College of Computing
Nathir Rawashdeh
narawash@mtu.edu

Michigan Technological University College of Computing https://orcid.org/0000-0002-9118-9317

Research Article

Keywords: PCB inspection, machine vision, AI segmentation, FANUC LR Mate 200iC, Siemens S7-1200, PROFINET, Ethernet/IP, FIFO, Ignition SCADA, industrial automation, few-shot learning.

Posted Date: October 1st, 2026

DOI: https://doi.org/10.21203/rs.3.rs-11087942/v1

License: This work is licensed under a Creative Commons Attribution 4.0 International License.
Read Full License

AI-Based Inline PCB Defect Detection and Robotic Sorting Using Smart Vision, PLC Logic, Fanuc Vision and SCADA Integration

Mizengo Abel Kabwe[1], Jacob Fata[1],
Ikerbold Nyasha Muzanenhamo[1], Cecil Takunda Mhike[1],
Nathir Rawashdeh[1*]

[1]Department of Electrical, Computer, and Mechatronics Engineering, Michigan Technological University, Houghton, MI, USA.

*Corresponding author(s). E-mail(s): narawash@mtu.edu;
Contributing authors: amkabwe@mtu.edu; mfata@mtu.edu;
inmuzane@mtu.edu; ctmhike@mtu.edu;

Abstract

This paper presents an AI-driven inline inspection system for PCB components, integrating the Overview OV20i smart camera, a Siemens S7-1200 PLC, and Ignition Perspective SCADA within a live manufacturing workcell. A FIFO based result management scheme within the PLC maintains synchronisation between vision decisions and physical part flow, ensuring each board is sorted according to its own inspection record even when multiple parts are simultaneously in transit on the conveyor. The architecture supports both Siemens and Allen-Bradley PLC environments, reflecting the mixed-vendor reality of most industrial automation facilities. Experimental validation across three test categories classification accuracy, orientation robustness, and lighting variation each returned 80% accuracy at prototype scale, confirming the suitability of the proposed architecture for inline industrial inspection applications.

Keywords: PCB inspection, machine vision, AI segmentation, FANUC LR Mate 200iC, Siemens S7-1200, PROFINET, Ethernet/IP, FIFO, Ignition SCADA, industrial automation, few-shot learning.

1 Introduction

Across electronics and semiconductor production lines, machine vision is steadily replacing manual inspection as the primary method for catching component level defects. The appeal of automated inspection lies not just in speed, but in consistency. The Ovi camera applies the same decision criteria to the first board of the day and the ten-thousandth, without fatigue or distraction.

Traditional rule based automated optical inspection (AOI) systems have been available for some time, yet they demand extensive manual programming and tend to struggle whenever parts shift position slightly or illumination drifts. Embedded AI inference changes this dynamic considerably. By training a segmentation model directly on representative images of both good and defective boards, the system learns to generalise across minor positional and lighting variations without requiring an engineer to rewrite detection rules for every new condition. When the camera level intelligence is connected to a PLC for sequencing and an industrial robot for physical sorting, the result is a fully automated inline workcell capable of detecting, classifying, and removing defective boards without any operator involvement in the nominal production flow.

This work describes such a system, built from commercially available industrial hardware and validated through structured laboratory trials.

2 Literature Review

Printed circuit board (PCB) inspection has become increasingly important as modern electronic systems continue to increase in complexity while decreasing in physical size. As component density rises and manufacturing tolerances become tighter, traditional quality assurance methods such as manual visual inspection are no longer sufficient for high-speed, repeatable, and reliable defect detection. Manual inspection is inherently subjective, labor intensive, and susceptible to operator fatigue, which makes it unsuitable for modern electronics production lines that demand consistent detection of missing components, soldering issues, trace defects, and placement errors [1, 2].To improve consistency and throughput, the electronics industry widely adopted Automated Optical Inspection (AOI), which uses machine vision and rule based image processing to identify visible PCB defects. Conventional AOI systems typically rely on template matching, image subtraction, thresholding, morphological operations, and geometric comparison against a known reference board. These methods perform adequately for obvious and repetitive defects, particularly in bare board inspection. However, their performance degrades when illumination changes, component positions shift slightly, or PCB orientation varies. In assembled PCB inspection (PCBA), these limitations become more significant because component presence, orientation, and solder quality create more complex visual conditions than bare copper defects alone. As a result, traditional AOI often suffers from false positives, limited adaptability, and frequent returning requirements whenever a new product is introduced [1, 2].Before the rise of deep learning, several researchers explored classical machine learning techniques such as support vector machines (SVMs), k-nearest neighbors, and feature based classifiers to improve inspection accuracy beyond rule based AOI. These approaches offered improved classification performance by learning from labeled

examples instead of depending entirely on hard coded rules. However, they still relied heavily on handcrafted features such as edge descriptors, texture statistics, or shape measurements. This dependency limited their robustness in real manufacturing environments where lighting, part positioning, and defect appearance can vary significantly from one board to another [1].Recent advances in deep learning, particularly convolutional neural networks (CNNs), have significantly improved PCB defect detection by enabling end-to-end feature learning directly from image data. Unlike traditional AOI systems, CNNs automatically learn hierarchical visual features that capture both low level patterns, such as edges and corners, and higher level defect structures, such as missing components, broken traces, solder bridges, and misalignments. A recent review of machine vision-based PCB defect detection methods confirms that the field has evolved from image processing-based approaches to machine learning and finally to deep learning-based methods, with deep learning currently offering the best overall performance for complex and small defect detection tasks [1].

The literature consistently shows that CNN based methods outperform conventional AOI in both accuracy and robustness. In Automated Defect Detection in Printed Circuit Boards: Exploring the Impact of Convolutional Neural Networks on Quality Assurance and Environmental Sustainability in Manufacturing, Ghelani reported that CNN based inspection could achieve approximately 98.2% accuracy while reducing dependence on manual re-inspection and improving inspection reliability in complex PCB manufacturing environments [2]. The study also emphasized that deep learning-based inspection can reduce waste and improve sustainability by lowering false rejects and minimizing unnecessary rework [2].

Similarly, in Implementation of an Automated PCB Defect Detection and Classification System, a CNN based automated visual inspection (AVI) framework was trained on 10,000 annotated PCB images and achieved an overall accuracy of 98.4%, with precision of 97.2%, recall of 96.8%, F1 score of 97.0%, and an average inspection time of 0.18 seconds per image. The system was based on a YOLOv4 architecture, selected for its balance between speed and accuracy, making it suitable for inline industrial deployment where high throughput is required [3]. These findings reinforce the practical value of one-stage object detectors for real time production environments.

In contrast to one-stage detectors, two-stage detectors such as Faster R CNN have also demonstrated strong performance in PCB defect detection where precise localization is required. In AI Driven Defect Detection in PCB Manufacturing: A Computer Vision Approach Using Convolutional Neural Networks, a Faster R CNN model with a ResNet 50 backbone was applied to detect defects such as missing holes, shorts, mouse bites, and spurious copper. The study reported mean average precision (mAP) of approximately 95% and highlighted the advantages of two stage architectures in accurately localizing small defects and reducing false detections [4]. Although these models are generally slower than YOLO style detectors, they remain highly relevant for applications where detection precision is more critical than raw inference speed [4].

Another important theme in the literature is the growing emphasis on dataset quality, augmentation, and defect diversity. Modern PCB inspection systems require sufficiently large and well annotated datasets to generalize effectively across multiple defect classes and variable operating conditions. The recent review by He et al. identified

publicly available datasets and categorized PCB defect detection methods into image processing-based, machine learning based, and deep learning based approaches. The authors also noted that current research is increasingly focused on lightweight models, Transformer based architectures, hybrid CNN Transformer networks, and practical industrial deployment constraints such as edge computing and real time inference [1]. These observations are important because they highlight that high benchmark accuracy alone does not guarantee industrial suitability.

A recurring limitation in the literature is that many high performing models are demonstrated in offline laboratory settings but are not fully integrated into a deterministic industrial control system. In many published studies, the focus is placed primarily on image classification or defect localization accuracy, with limited attention to how inspection results are synchronized with moving products, communicated to controllers, or used for automated reject handling on a live production line [1, 4]. This gap is particularly relevant in manufacturing, where a vision result is only useful if it can be reliably linked to the correct physical part at the correct time.

This gap is directly addressed by the present project, AI-Based Inline PCB Defect Detection and Robotic Sorting Using Smart Vision, PLC Logic, and SCADA Integration, which extends beyond standalone AI inspection by embedding machine vision into a complete industrial workcell. The proposed system integrates an Overview OV20i smart camera, a Siemens S7-1200 PLC, a FANUC LR Mate 200iC industrial robot, and Ignition Perspective SCADA within a live inline conveyor environment [5]. Rather than using external GPU based inference only, the project leverages segmentation based inspection on the smart camera itself, making the inspection decision directly available to the PLC in a practical automation ready form [5].

A key contribution of the project, relative to much of the prior literature, is the implementation of a FIFO based result management strategy within the PLC. In inline inspection systems, multiple boards may be in transit simultaneously between the camera station and the sorting station. Without proper synchronization, inspection results can easily be applied to the wrong board. In this project, the first photoelectric sensor triggers the OV20i inspection, and the PLC stores the resulting PASS/FAIL decision in a software FIFO queue. When the same board reaches the second sensor at the robot pick station, the PLC pops the corresponding inspection result from the queue and issues the correct sorting command. This ensures deterministic alignment between vision decisions and physical part flow, even when multiple PCBs are moving through the conveyor system [5]. This is a strong practical contribution because synchronization challenges are often overlooked in purely algorithmic PCB defect detection research.

The project also demonstrates a realistic multi protocol industrial communication architecture. The OV20i camera communicates with the Siemens S7-1200 via PROFINET, allowing cyclic exchange of inspection data and trigger signals. The PLC then communicates with the FANUC robot over EtherNet/IP using an LCCF scanner block, while Ignition SCADA connects through OPC-UA for real time monitoring, data logging, and operator visibility [5]. This mixed vendor, multi protocol design reflects actual industrial practice more closely than many academic demonstrations, which often omit the control layer and supervisory integration required for deployment.

Experimental validation of the project showed that the prototype system achieved 80% accuracy across three test categories: classification accuracy, orientation robustness, and lighting variation [5]. While this is lower than the 95%–98% accuracy reported in large-dataset deep learning studies [2, 4], the result should be interpreted in context. The present project is not simply an offline CNN benchmark; it is a prototype scale cyber physical inspection cell built using commercially available industrial hardware, few shot AI training, PLC logic, robotic sorting, and SCADA supervision. Its contribution lies in demonstrating the feasibility of end-to-end inline AI inspection and automated sorting, rather than solely maximizing model accuracy under controlled dataset conditions [5].

Overall, the literature indicates that PCB inspection has evolved from manual and rule based AOI methods to advanced AI driven machine vision systems, with CNN based and segmentation based approaches offering clear advantages in defect adaptability, robustness, and scalability [1, 4]. However, there remains a significant gap between high-performing research models and fully integrated industrial workcells capable of deterministic sequencing, communication, automated rejection, and supervisory visibility. The present project contributes to closing that gap by combining embedded AI vision, PLC based sequencing, robotic sorting, and SCADA integration into a practical inline inspection platform aligned with Industry 4.0 manufacturing principles [5].

3 System Architecture Overview

The workcell is structured across four interdependent functional layers. The vision AI layer performs embedded inference directly on the camera hardware. The PLC control layer sequences the process and manages inspection results. The material handling layer transports and positions parts along the conveyor.

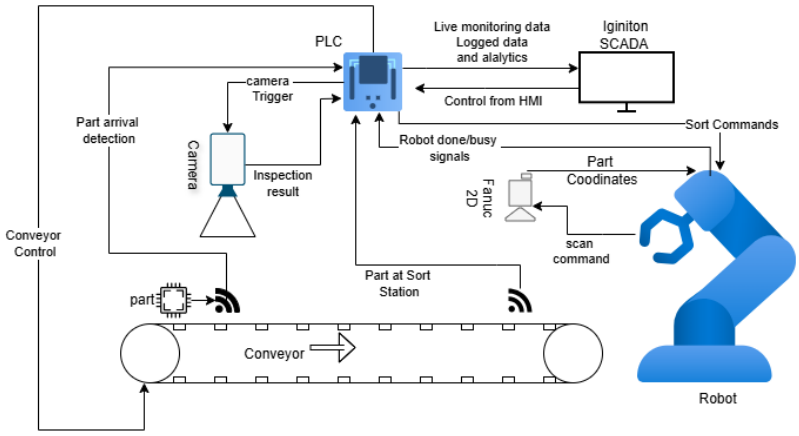


Fig. 1 System architecture overview.

The supervisory SCADA layer monitors and logs the entire operation in real time. Each layer communicates with adjacent layers through well defined industrial protocols,

keeping functional boundaries clean and the overall architecture straightforward to extend or modify.

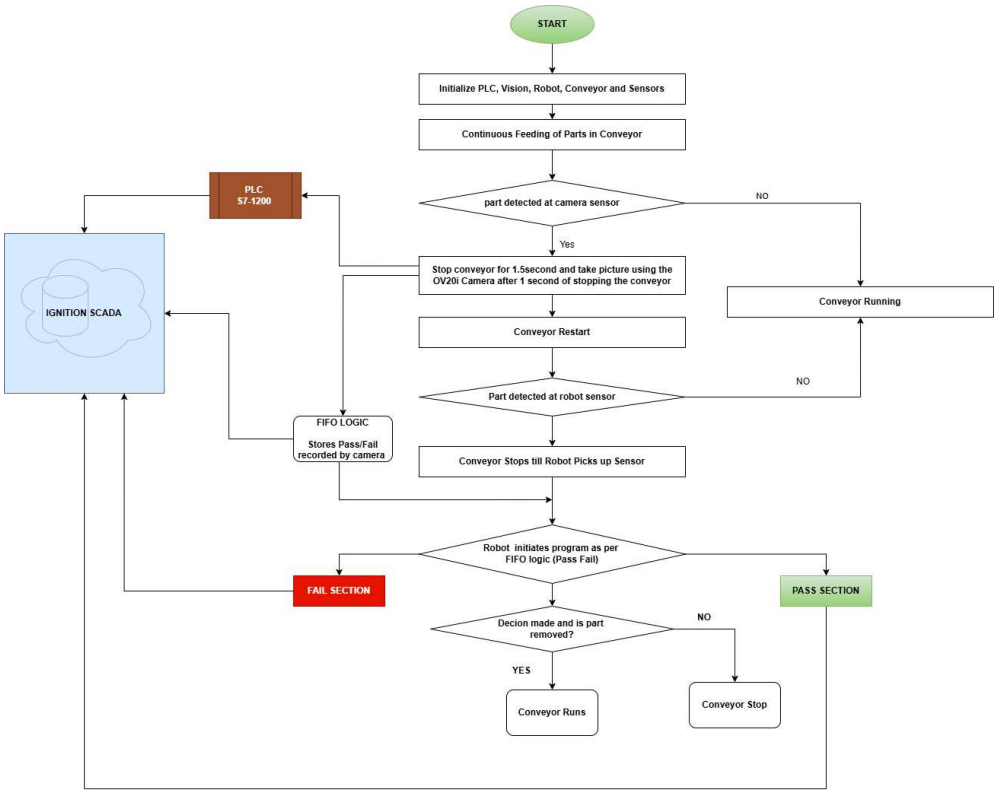


Fig. 2 PLC sequence flowchart illustrating sensor-triggered inspection, FIFO result latching, and conditional robot sorting command issuance.

3.1 Electrical Architecture

The electrical distribution originates from a 120 VAC mains supply. A 24 VDC switched mode power supply branches from this source to power the Siemens S7-1200 PLC, both photoelectric sensors, and all associated digital I/O devices. A separate branch from the mains feeds the conveyor motor drive. This arrangement isolates the low-voltage control circuitry from the motor drive, reducing noise coupling into sensor lines and communication interfaces, a particularly important consideration when operating high-resolution vision hardware alongside variable speed motor drives.

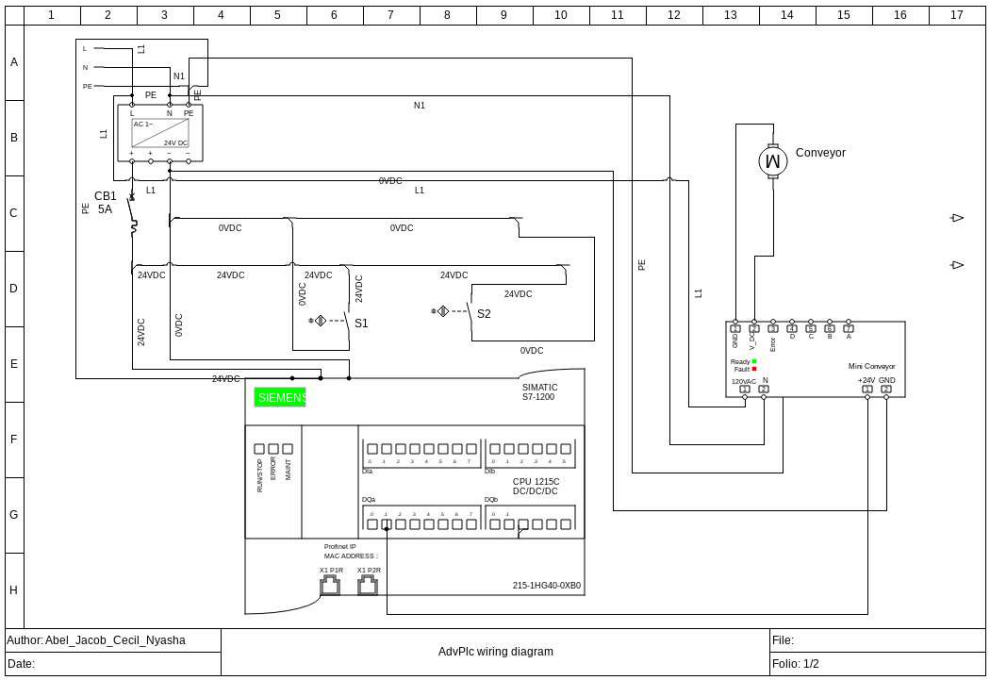


Fig. 3 Electrical schematic showing 120 VAC mains distribution, 24 VDC control supply, and conveyor motor drive branch.

3.2 Communication Architecture

All network capable devices share a single five port industrial Ethernet switch, forming one flat network segment. Three distinct protocols operate across this shared physical infrastructure, each handling a specific device relationship.

PROFINET (OV20i ↔ S7-1200): The OV20i camera integrates into the PROFINET device network using a GSD file imported into TIA Portal. This allows the PLC to trigger image capture and receive structured inspection data including segmentation blob counts and the resulting pass/fail decision through cyclic PROFINET I/O exchanges.

EtherNet/IP (S7-1200 ↔ FANUC controller): An LCCF EtherNet/IP scanner block on the PLC side exchanges tag data with the FANUC robot controller. The PLC sends sorting commands and inspection outcomes; the robot controller returns status and handshake signals.

OPC-UA (S7-1200 ↔ Ignition SCADA): An OPC-UA connection exposes PLC tags to the Ignition server, enabling real-time monitoring and historian logging without introducing polling delays.

Because PROFINET and EtherNet/IP carry data in incompatible formats, a dedicated data-mapping conversion block within the PLC program translates between the two protocol domains, ensuring consistent information exchange across the mixed-vendor hardware environment without requiring external gateways.

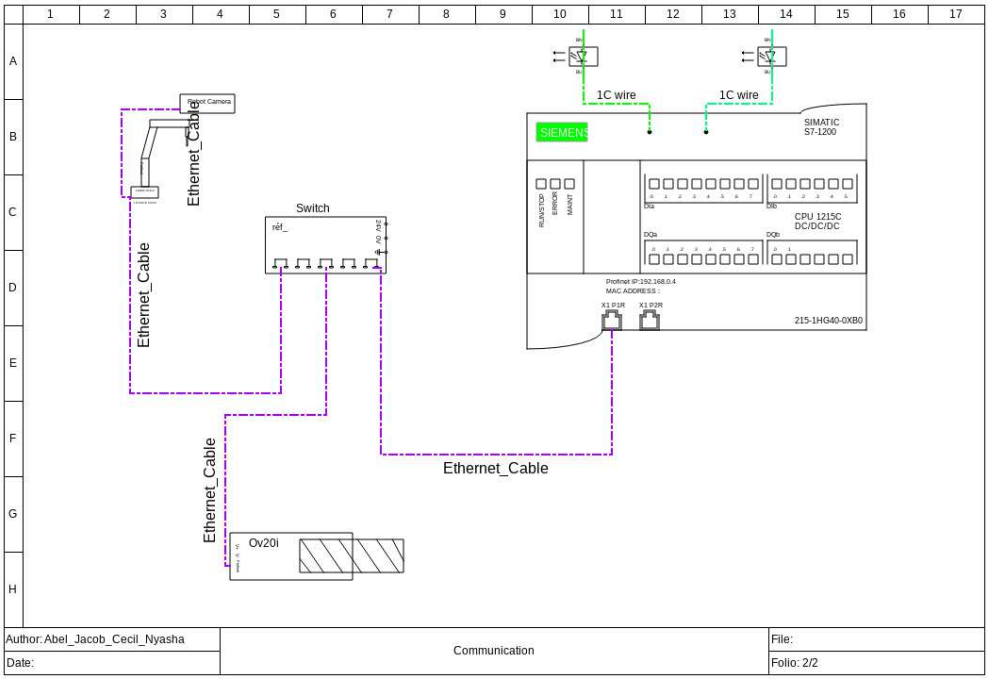


Fig. 4 Communication architecture showing PROFINET camera integration, EtherNet/IP robot control, and OPC-UA SCADA connection.

4 System Implementation

4.1 Hardware Configuration

Figure 5 shows the integrated automated sorting workstation used in the project. The system combines a Siemens PLC, an AI vision camera, a robotic manipulator, a belt conveyor, and photoelectric sensors to detect, inspect, classify, and sort parts in real time.

4.1.1 Siemens S7-1200 CPU 1214C DC/DC/DC PLC

The Siemens S7-1200 PLC serves as the central controller of the automation system. It receives input signals from the photoelectric sensors and the vision system, executes the control logic, and sends output commands to coordinate conveyor motion and robot triggering.

Function: Main control and sequencing unit

Role in project: Handles sensor logic, inspection timing, and robot/conveyor coordination

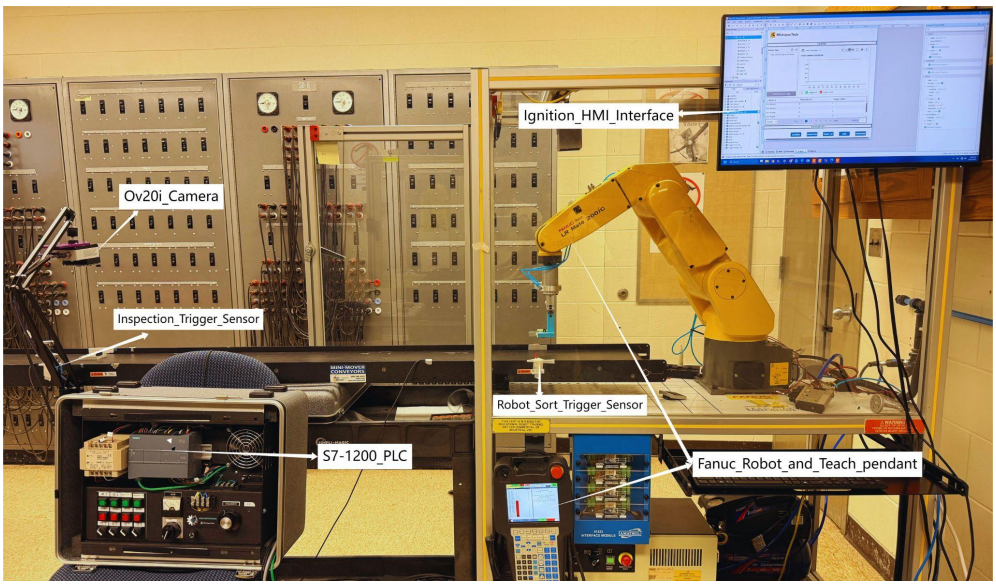


Fig. 5 Physical workcell showing the conveyor, OV20i camera inspection station, photoelectric sensors, and FANUC LR Mate 200iC robot with custom end-of-arm gripper.

4.1.2 Overview AI OV20i Smart Camera (Advantech ICAM-520-10W Platform)

The Overview AI OV20i smart camera, running on the Advantech ICAM-520-10W industrial vision platform, is used for part inspection and classification. It captures images of objects on the conveyor and applies trained AI-based inspection models to determine whether the part is Pass/Fail or whether a defect is present.

4.1.3 Robot System and End-of-Arm Tooling

The FANUC LR Mate 200iC handles all physical sorting operations based on commands received from the PLC over EtherNet/IP.

A custom end-of-arm gripper was designed and fabricated specifically to handle PCB panels securely without risk of component damage during the pick-and-place cycle. Before each pick, the onboard FANUC 2D grayscale vision system captures an image at the pick station to determine the board's precise position and orientation, applying a calculated visual offset to the nominal pick point to compensate for any residual positional variation introduced by the conveyor stop mechanism.

4.1.4 Belt Conveyor Transport System with Adjustable Speed

The belt conveyor system transports parts through the inspection and sorting zones. Its adjustable speed allows the system to be tuned for proper synchronization between the camera, sensors, PLC, and robot.

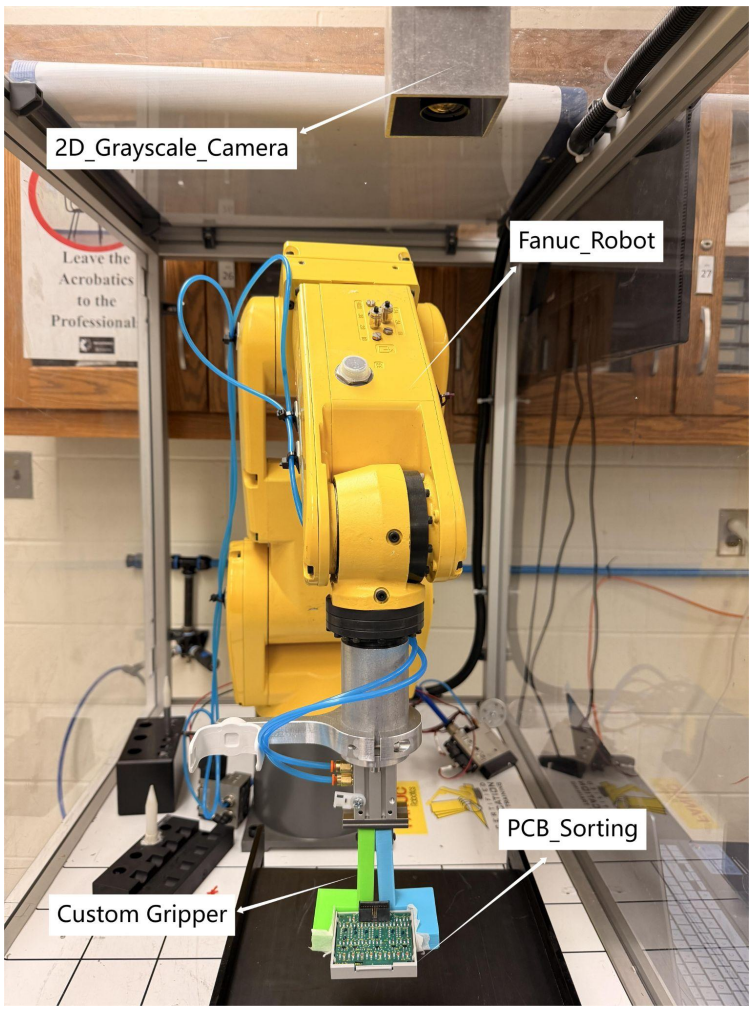


Fig. 6 FANUC LR Mate 200iC at the robot pick station, showing the custom gripper, accept conveyor lane, and reject bin placement zones.

4.1.5 Photoelectric Sensor Integration

Two ML17-54/115/136 photoelectric sensors are mounted along the conveyor at fixed stations. Both sensors are wired in PNP Normally Closed (NC) mode through the white output lead, sourcing 24 VDC signals to the sinking digital inputs of the S7-1200. The first sensor, mounted directly beneath the OV20i camera, detects part arrival at the inspection station and initiates the stop inspect resume cycle. The second sensor, located at the robot pick station, detects the same part after transport and triggers the sorting routine.

4.1.6 SCADA Integration

Ignition Perspective SCADA provides continuous supervisory monitoring through a custom HMI screen developed specifically for this workcell. The display shows real-time states of both photoelectric sensors, conveyor run/stop status, the current inspection result from the OV20i, robot operational status, and running cumulative totals of accepted and rejected boards.

The ability to see all subsystem states simultaneously on a single screen shortened fault identification time substantially during the integration phase.



Fig. 7 Ignition Perspective SCADA interface showing real-time sensor states, conveyor status, inspection result (PASS/FAIL), and robot operational status during live workcell operation.

4.1.7 Two ML17-54/115/136 PNP Photoelectric Sensors (24 VDC, NC Output)

The two ML17-54/115/136 PNP photoelectric sensors are used as position and trigger sensors in the system. One sensor is placed near the camera to trigger image capture, while the other is placed near the robot pickup area to trigger the robot sorting sequence. Since they are 24 VDC PNP normally closed (NC) devices, they provide a sourcing output to the PLC input circuit

4.2 Vision System and Camera Training

The OV20i was configured for segmentation based inspection rather than image level classification. Segmentation was chosen specifically because it retains per pixel spatial information.This allows the model to localise missing or displaced IC sites within the camera's field of view regardless of minor positional shifts or moderate part rotation.

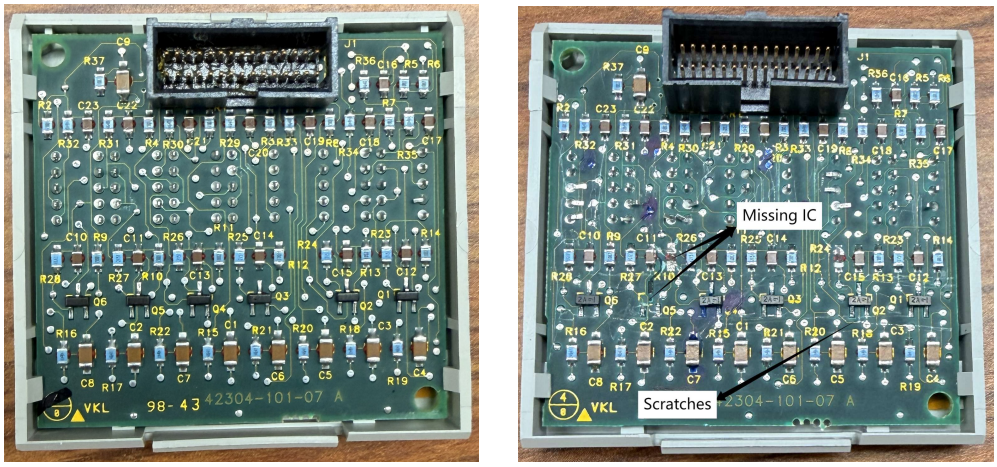


Fig. 8 PCB inspection examples: good board (left) and defective board with missing ICs and scratches (right).

A representative dataset of labeled printed circuit board (PCB) images was acquired under nominal workcell lighting conditions to capture realistic operational variability.

The trained model was configured to classify two distinct categories: pass_missing_ics, corresponding to correctly populated integrated circuit (IC) locations, and fail_missing_ics, representing regions where ICs are absent or improperly positioned. During runtime, the model generates segmentation outputs in the form of blobs, where each blob corresponds to a spatial region associated with one of the predefined classes.A pictorial view of part of the annotations that were used for training of the bad parts is shown below.

Within the OV20i gateway interface, a Node RED based processing pipeline is employed to interpret the inference results. Specifically, a function node parses the incoming message payload, extracts the predicted class labels, and computes the

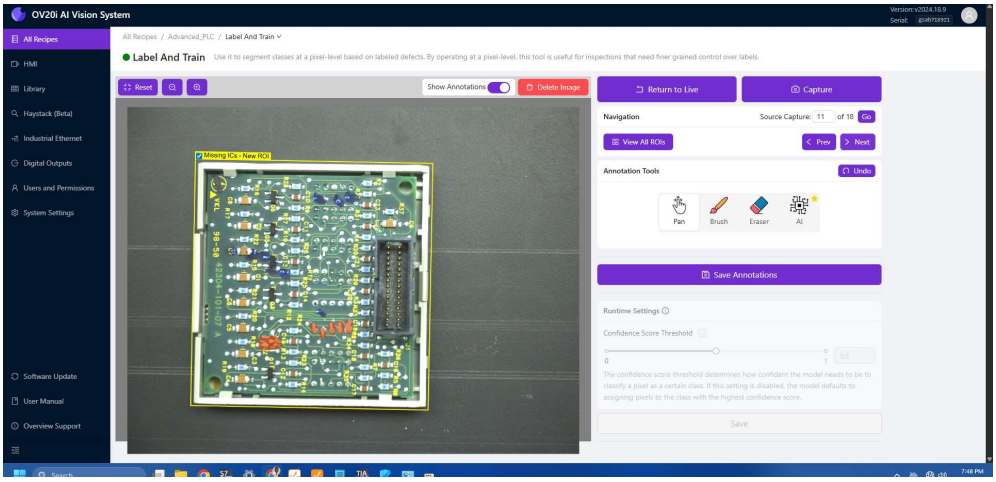


Fig. 9 Example defect annotations used to train the segmentation model.

number of blobs associated with each class. The inspection decision is then derived using deterministic logic; the presence of one or more fail_missing_ics blobs results in a FAIL classification, whereas the absence of such blobs yields a PASS classification. This decision is subsequently transmitted to the programmable logic controller (PLC) for execution of downstream control actions, including conveyor actuation and robotic sorting.

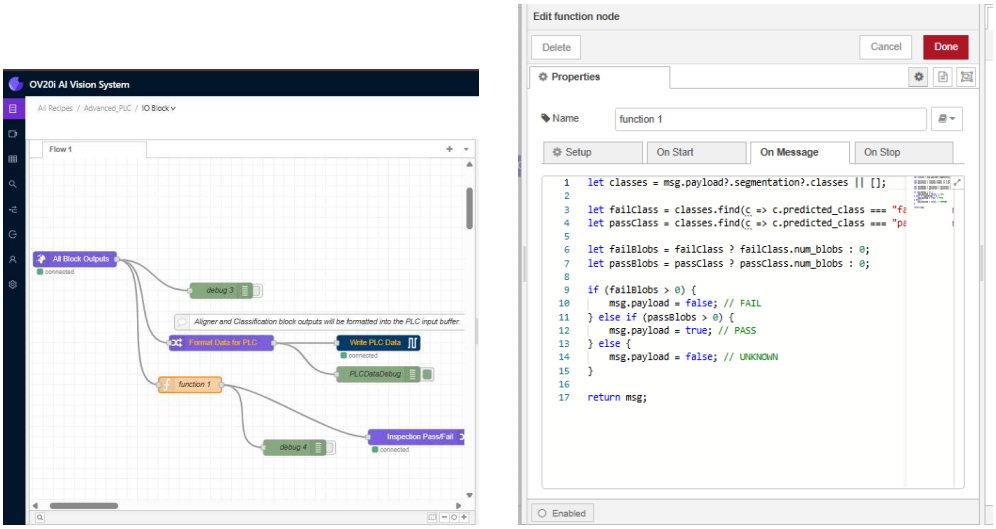


Fig. 10 Node-RED processing flow (left) and function used for blob analysis and pass/fail decisions (right).

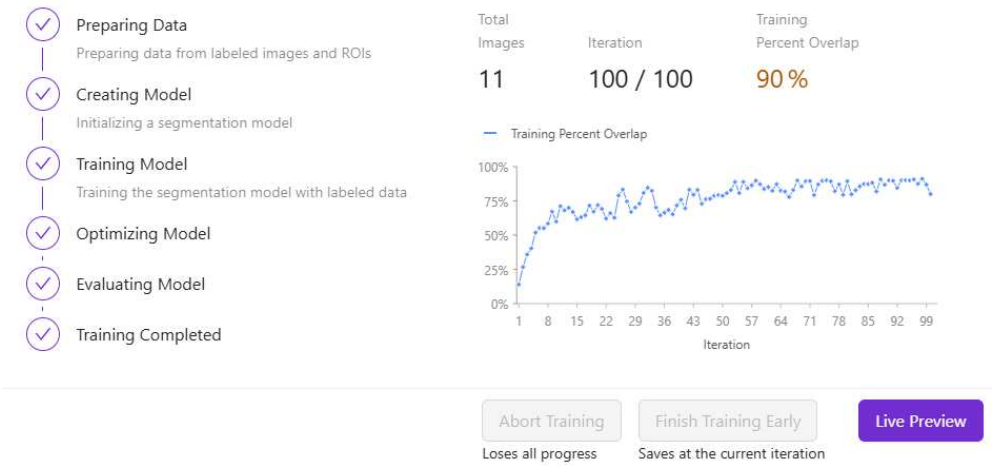


Fig. 11 Camera training workflow showing the few-shot labelled dataset, segmentation model training, and blob-based inference at runtime.

4.3 PLC Program and FIFO Result Management

The PLC program, developed in Siemens TIA Portal, coordinates the conveyor, camera trigger, and robot sorting sequence through an event driven state machine. A central design requirement was that boards enter the conveyor continuously, meaning two or more parts may be simultaneously travelling between the inspection station and the robot pick station at any given moment. To handle this correctly and prevent result misassignment, a software FIFO queue was implemented in the PLC.

When the first photoelectric sensor detects a board arriving at the camera station, the conveyor stops and the PLC triggers image capture. Once the OV20i returns its inspection result within approximately one second of capture the PLC pushes the PASS or FAIL outcome onto the tail of the FIFO queue and restarts the conveyor. When the second sensor detects that same board arriving at the robot pick station, the PLC pops the oldest entry from the head of the FIFO and uses that result to issue the sorting command to the robot. Because results enter and leave the FIFO in strict first-in, first-out order, each board is always sorted according to its own inspection record, even when multiple boards are simultaneously in transit.

The conveyor dwell time at the inspection station is set to 1.5 seconds, providing a 0.5-second margin beyond the camera's worst-case inference time before motion resumes. This margin prevents false triggers and ensures a stable image is captured before the conveyor restarts.

5 Results and Discussion

5.1 Inspection Performance Under Normal Lighting

A total of 14 PCB samples were inspected under normal ambient lighting conditions using the OV20i AI Vision System configured for missing IC detection. The system classified 7 boards as PASS and 7 boards as FAIL across 14 recorded captures. The

cumulative system yield at the close of the inspection session stood at 31.91%, consistent with the expected proportion of defective boards in the test batch.

Table 1 Individual sample inspection results (normal lighting condition)

Sample #	Cap ID	Trigger ID	Result	Fail Blobs	Pass Blobs	Fail Area (px)	Align Conf (%)	Latency (ms)
1	202	144	FAIL	39	0	24,207	65.7	386
2	203	145	PASS	0	66	0	61.6	447
3	205	147	FAIL	9	0	4,701.5	68.8	308
4	206	148	FAIL	10	0	4,252	74.6	578
5	207	149	FAIL	2	0	1,915	91.2	555
6	208	150	FAIL	48	0	8,797	68.2	367
7	209	151	FAIL	39	0	23,481.5	52.4	370
8	210	152	PASS	0	64	0	58.1	426
9	212	154	PASS	0	66	0	54.7	412
10	213	155	PASS	0	66	0	61.6	419
11	214	156	PASS	0	65	0	62.5	726
12	215	157	PASS	0	66	0	57.0	413
13	216	158	PASS	0	66	0	60.0	445
14	217	159	PASS	0	66	0	56.3	679

Table 2 Summary statistics of normal lighting condition (14 confirmed samples)

Metric	Value
Total samples inspected	14
Boards classified PASS	8
Boards classified FAIL	7
Session pass rate (this experiment)	53.3% (8/15 visible)
Cumulative yield at session end (Cap 218)	31.91%
Cumulative total inspections (system counter)	141
Cumulative passed (system counter)	45
Cumulative failed (system counter)	96
confirmed experiment pass total	38
confirmed experiment fail total	93
Alignment confidence range (%)	51.9 – 91.2
Alignment confidence mean (%)	63.0
System latency range (ms)	308 – 726
System latency mean (ms)	482

5.2 Blob Detection Analysis

The primary detection metric employed by the system is blob analysis within a defined Region of Interest (ROI). On PASS boards, the system consistently identified between

64 and 66 pass-classified blobs, corresponding to the expected number of IC footprints populated on the board. The mean total pass blob area was approximately 32,579 pixels, indicating a stable and repeatable detection signature for correctly assembled boards.

Table 3 Pass sample blob statistics

Sample	Cap ID	Pass Blobs (#)	Total Pass Area (px)	Align Conf (%)
2	203	66	32,194	61.6
8	210	64	37,817	58.1
9	212	66	32,102	54.7
10	213	66	33,716.5	61.6
11	214	65	34,830	62.5
12	215	66	32,102	57.0
13	216	66	33,835	60.0
14	217	66	24,033	56.3
Mean		65.6	32,579	58.975

On FAIL boards, fail blob counts ranged widely from 1 (Capture 218) to 48 (Capture 208), with a mean of 21.1 fail blobs per defective board. This variability is significant. Capture 208 presented 48 fail blobs with a comparatively low total area of 8,797 pixels, suggesting the presence of numerous small, low-confidence detections that may reflect noise, partial component presence, or solder residue rather than fully absent ICs. By contrast, Captures 202 and 209 each recorded approximately 39 fail blobs with large cumulative areas exceeding 23,000 pixels, more consistent with genuinely missing IC clusters. This distinction highlights the importance of setting an appropriate confidence score threshold currently set to "None" which, when left unconfigured, may increase the false positive rate for marginal defect cases.

Table 4 Failed sample blob statistics

Sample	Cap ID	Fail Blobs (#)	Total Fail Area (px)	Max Blob Area (px)	Max Major Axis (px)
1	202	39	24,207	1,134.5	63.0
3	205	9	4,701.5	1,041.5	60.0
4	206	10	4,252	1,062	57.0
5	207	2	1,915	1,026.5	48.0
6	208	48	8,797	529	33.0
7	209	39	23,481.5	1,152.5	60.5
15*(extra)	218	1	459.5	459.5	42.0
Mean		21.1	9,687.6	—	—
Total		148	67,814	—	—

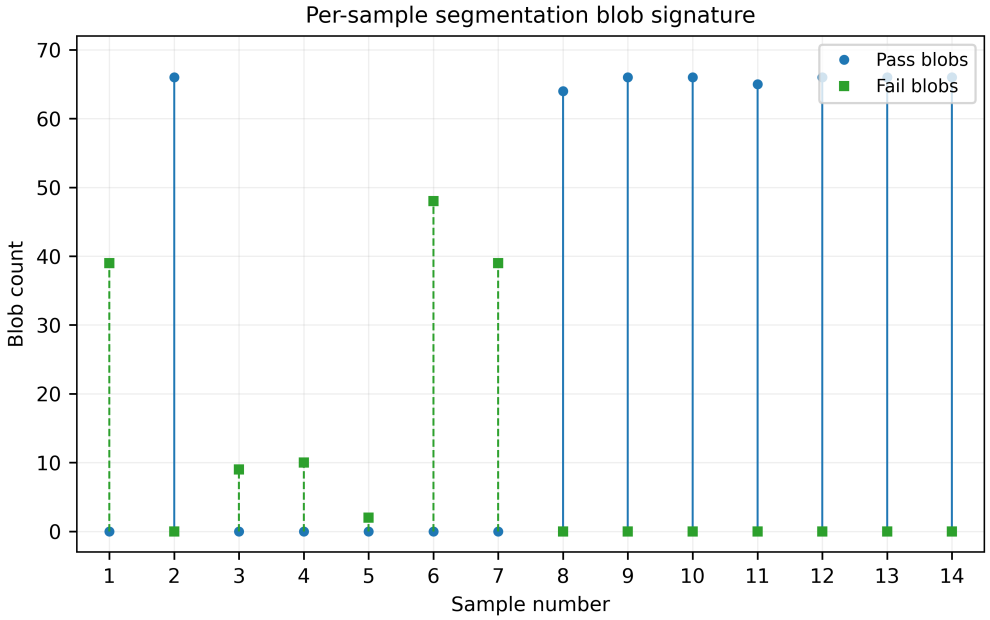


Fig. 12 Blob count vs. sample number for the 14 inspection records in Table 1.

5.3 Alignment Confidence Analysis

Alignment confidence varied between 51.9% and 91.2% across all samples. Importantly, Capture 207 recorded the highest alignment confidence in the dataset (91.2%) yet still yielded a FAIL result with 2 detected fail blobs. This finding demonstrates that alignment confidence alone is not a reliable proxy for inspection correctness. The moderate confidence values observed across most samples (mean 63.0%) suggest that board-to-board positional variation likely due to manual placement or fixture tolerances is a consistent factor. Improving fixturing to ensure repeatable board positioning would be expected to raise alignment confidence and reduce ambiguous detections.

Table 5 Alignment confidence vs. inspection result

Confidence Band	PASS count	FAIL count	Total	FAIL rate (%)
$\geq 80\%$	0	1	1	100%
60 – 79.9%	5	3	8	37.5%
50 – 59.9%	3	3	6	50.0%
$< 50\%$	0	0	0	—
All samples	8	7	15	46.7%

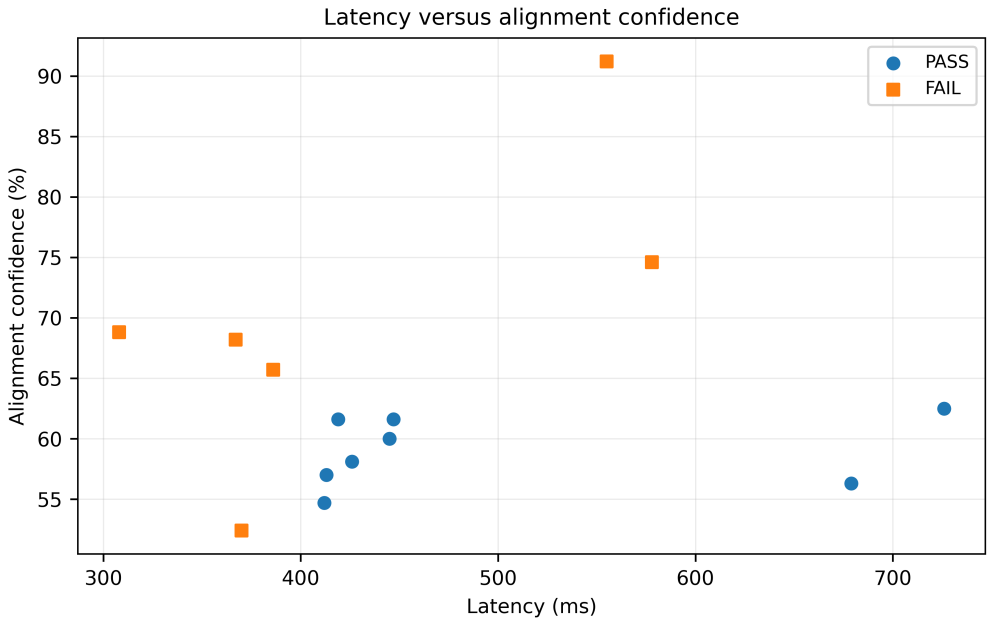


Fig. 13 Alignment confidence vs. latency for the 14 inspection records in Table 1.

5.4 System Latency

Mean system latency across all samples was 482 ms, with a range of 308–726 ms. No meaningful correlation was observed between latency and inspection outcome (PASS mean: 508 ms; FAIL mean: 451 ms). All latency values are operationally acceptable for an inline inspection context, though optimisation of lighting and image acquisition hardware could reduce upper-bound latency for high-throughput production environments.

Table 6 System latency summary

Condition	Min (ms)	Max (ms)	Mean (ms)
PASS samples (n=8)	412	726	508
FAIL samples (n=7)	308	693	451
All samples (n=15)	308	726	482

5.5 Conveyor and Sensor Synchronisation

The two-sensor stop and go architecture proved entirely reliable throughout testing. The inspection-station sensor consistently halted each board within the OV20i camera's calibrated field of view, and the pick-station sensor consistently positioned each board within the FANUC robot's reachable workspace. No FIFO overwrite incidents were recorded across all multi-board transit scenarios, confirming that the result-latching scheme maintained strict part-to-result integrity throughout every test run.

The stop and go strategy simplifies PLC logic compared with continuous-motion tracking but inherently limits throughput to one inspection cycle per conveyor dwell interval. This trade-off is well-suited to the prototype scale of this implementation but warrants re-evaluation if the architecture is scaled to higher volume production lines.

5.6 Robot Sorting Performance

The FANUC LR Mate 200iC executed pick-and-place sorting operations reliably throughout the entire test campaign. Sorting was conditioned on both confirmed part presence at the second sensor and the availability of a valid inspection result at the head of the FIFO, preventing any spurious robot motion in ambiguous or transitional states. The FANUC 2D vision system successfully compensated for residual positional variation at the pick station in all observed trials, confirming that vision guided picking adds meaningful and measurable robustness beyond fixed position pick routines. Zero EtherNet/IP handshake failures were recorded across all sorting cycles, confirming stable and deterministic PLC to robot communication over the full duration of testing.

5.7 SCADA Monitoring Performance

The Ignition Perspective interface provided uninterrupted real-time visibility throughout all test sessions. Operators were able to verify sensor states, conveyor status, and inspection outcomes at a glance, without needing to open the PLC programmer or robot teach pendant. Table 7 summarises the monitoring parameters implemented and their update behaviour.

Table 7 SCADA monitoring functions

Monitored Parameter	Update Mode
Sensor 1 — inspection station state	Cyclic (OPC-UA)
Sensor 2 — robot pick station state	Cyclic (OPC-UA)
Conveyor run / stop status	Cyclic (OPC-UA)
Inspection result (PASS / FAIL)	Event-driven
Robot status and current action	Cyclic (OPC-UA)
Cumulative pass count	Event-driven
Cumulative fail count	Event-driven

The layered update strategy cyclic polling for continuous states, event driven updates for discrete inspection outcomes kept OPC-UA traffic low while ensuring

that inspection results appeared on the display without any perceptible delay. This approach proved particularly useful during commissioning for isolating the source of sequencing faults across the four system layers.

6 Conclusion

This project demonstrated the end-to-end design, integration, and experimental validation of an AI-based inline PCB inspection and sorting workcell. The system brought together an Overview OV20i segmentation based smart camera, a Siemens S7-1200 PLC with FIFO-based result management, a FANUC LR Mate 200iC robot with onboard vision-guided picking, and Ignition Perspective SCADA monitoring all operating as a coordinated, single-network automation platform.

This study also evaluated the OV20i AI Vision System for automated detection of missing integrated circuits on PCB assemblies under normal ambient lighting conditions. The system demonstrated a clear ability to discriminate between populated and unpopulated IC footprints using blob-based classification, consistently detecting 64–66 pass blobs on correctly assembled boards. Defective boards exhibited highly variable blob counts (1–48), underscoring the need for threshold calibration to minimise false detections arising from noise or partial component presence.

The overall session yield of 31.91% reflects the composition of the test batch rather than a system limitation. Alignment confidence, while a useful diagnostic indicator, was found to be an insufficient standalone predictor of inspection outcome. The system latency of 308–726 ms is compatible with semi-automated inspection workflows.

The results further confirms that a layered AI-vision and PLC controlled automation architecture is a practical and extensible approach for inline PCB quality inspection. To advance this system from laboratory demonstration toward industrial deployment, future work should focus on expanding the training dataset to cover a wider range of orientations, lighting conditions, and defect types.

The FIFO result latching scheme operated without a single overwrite incident throughout all multi board transit tests, confirming that the synchronisation architecture correctly decouples inspection timing from physical transport delay. Zero EtherNet/IP communication faults were recorded during robot sorting, and the SCADA layer provided genuinely useful fault isolation during commissioning.

6.1 System Limitations

Three practical limitations were identified during evaluation. First, inspection accuracy was sensitive to positioning repeatability, boards that stopped even slightly outside the camera's calibrated field of view produced inconsistent segmentation outputs that degraded classification reliability.

Second, the stop and go conveyor strategy constrains throughput to one inspection cycle per dwell interval, a trade off that is manageable at prototype scale but requires re-examination for higher volume production applications.

Third, the training dataset was limited in both overall size and angular diversity, which accounts directly for the orientation and lighting failures observed in the results. Addressing these limitations through improved mechanical part guidance, a

substantially larger and more varied training dataset, and potentially a continuous motion inspection strategy represents the clearest path toward production readiness.

Declarations

Funding: Not applicable.
Clinical Trial Registration: Not applicable.
Ethics, Consent to Participate, and Consent to Publish Declarations: None required.
Conflict of Interest: The authors declare no competing interests.
Data Availability Statement: The data generated during the current study are not publicly available due to their specific nature, but are available from the corresponding author on reasonable request.

References

[1] Z. He, Y. Lian, Y. Wang, and Z. Lu, "A comprehensive review of machine vision-based PCB surface defect detection methods," Results in Engineering, vol. 27, Art. no. 106437, 2025, doi: 10.1016/j.rineng.2025.106437.

[2] H. K. J. Ghelani, "Automated defect detection in printed circuit boards: Exploring the impact of convolutional neural networks on quality assurance and environmental sustainability in manufacturing," International Journal of Advanced Engineering Technologies and Innovations, vol. 1, no. 4, pp. 275–289, 2022.

[3] H. K. J. Ghelani, Implementation of an Automated PCB Defect Detection and Classification System, unpublished manuscript, 2025.

[4] K. Patel, "AI-driven defect detection in PCB manufacturing: A computer vision approach using convolutional neural networks," European Journal of Advances in Engineering and Technology, vol. 12, no. 6, pp. 10–25, 2025.

[5] C. T. Mhike, I. N. Muzanenhamo, M. A. Kabwe, J. Fata, and N. Rawashdeh, "AI-based inline PCB defect detection and robotic sorting using smart vision, PLC logic, and SCADA integration," unpublished manuscript, Michigan Technological University, 2026.

[6] Y. Wang and Y. Liu, "Automated visual inspection of printed circuit boards using deep learning," IEEE Transactions on Industrial Electronics, vol. 66, no. 12, pp. 9415–9426, 2019.

[7] B. Hu and J. Wang, "Detection of PCB surface defects with improved Faster R-CNN and feature pyramid network," IEEE Access, vol. 8, pp. 108335–108345, 2020.

[8] R. Ding, L. Dai, G. Li, and H. Liu, "TDD-net: A tiny defect detection network for printed circuit boards," CAAI Transactions on Intelligence Technology, vol. 4,

no. 2, pp. 110–116, Jun. 2019.

[9] H. G. Nguyen, T. T. Nguyen, and V. T. Tran, "Automated visual inspection for printed circuit board defect detection using convolutional neural networks," IEEE Access, vol. 10, pp. 31561–31573, 2022.

[10] X. Li, X. Ding, and J. Sun, "A survey on deep learning-based PCB defect detection methods," J. Manuf. Syst., vol. 68, pp. 334–352, Jul. 2023.

[11] Y. Liu et al., "Real-time PCB defect detection using lightweight YOLO models for industrial automation," Expert Syst. Appl., vol. 211, p. 118455, Jan. 2023.

[12] K. He, G. Gkioxari, P. Dollár, and R. Girshick, "Mask R-CNN," in Proc. IEEE Int. Conf. Comput. Vis. (ICCV), Venice, Italy, Oct. 2017, pp. 2961–2969.

[13] J. Long, E. Shelhamer, and T. Darrell, "Fully convolutional networks for semantic segmentation," in Proc. IEEE Conf. Comput. Vis. Pattern Recognit. (CVPR), Boston, MA, USA, Jun. 2015, pp. 3431–3440.

[14] International Electrotechnical Commission, IEC 61131-3: Programmable Controllers Part 3: Programming Languages, 3rd ed. IEC, Geneva, Switzerland, 2013.

[15] Siemens AG, S7-1200 Programmable Controller System Manual. Siemens, Nuremberg, Germany, 2021.

[16] FANUC America Corporation, LR Mate 200iC Mechanical Unit Operator's Manual. FANUC, Rochester Hills, MI, USA, 2012.

[17] Inductive Automation, Ignition Platform Documentation, 2023. [Online]. Available: https://docs.inductiveautomation.com

[18] Overview AI, OV20i Smart Camera User Guide, 2023. [Online]. Available: https://www.overview.ai

[19] Almtireen, Natheer, et al. "PLC-controlled intelligent conveyor system with AI-enhanced vision for efficient waste sorting." Applied Sciences 15.3 (2025): 1550.

[20] Li, Yu-Ting. Artificial Intelligence Technology in Image Inspection for Industrial 4.0 Applications. Diss. National Yang Ming Chiao Tung University, 2021.